Eur. Phys. J. B **18**, 49–54 (2000)

THE EUROPEAN PHYSICAL JOURNAL B

EDP Sciences

Anelastic relaxation and ^{139}La NQR in $La_{2-x}Sr_xCuO_4$ around the critical Sr content x = 0.02

A. Campana[1,a], R. Cantelli[2], F. Cordero[3], M. Corti[1], and A. Rigamonti[1]

[1] Dipartimento di Fisica "A. Volta" and Unitá INFM di Pavia, Via Bassi 6, 27100 Pavia, Italy
[2] Dipartimento di Fisica, Universitá di Roma "La Sapienza" and Unitá INFM, P.zale A. Moro 2, 00185 Roma, Italy
[3] CNR, Area di Ricerca di Roma-Tor Vergata, Istituto di Acustica "O.M. Corbino" and Unitá INFM, Via del Fosso del Cavaliere, 00133 Roma, Italy

Received 18 May 2000 and Received in final form 11 July 2000

Abstract. Anelastic relaxation and ^{139}LaNQR relaxation rates in $La_{2-x}Sr_xCuO_4$ for Sr content around 2 and 3 percent are discussed in terms of spin and lattice excitations and of the related ordering processes. It is argued how the phase diagram of $La_{2-x}Sr_xCuO_4$ at the boundary between the antiferromagnetic (AF) and the spin-glass phase ($x = 0.02$) could be more complicate than previously thought, with a transition to a quasi-long range ordered state at $T \simeq 150$ K, as indicated by neutron scattering data. On the other hand, the ^{139}LaNQR spectra are compatible with a transition to an AF phase around $T \simeq 50$ K, in agreement with the phase diagram commonly accepted in literature. In this case the peaks in NQR and anelastic relaxation rates around 150 K and 80 K respectively in $La_{1.98}Sr_{0.02}CuO_4$, yield the first evidence of freezing process involving simultaneously lattice and spin excitations, possibly corresponding to motion of charged stripes.

PACS. 74.25.Dw Superconductivity phase diagrams – 76.60.-k Nuclear magnetic resonance and relaxation – 62.40.+i Anelasticity, internal friction, stress relaxation, and mechanical resonances

1 Introduction

From a variety of recent experiments and theoretical descriptions (mostly motivated by the search of the microscopic mechanism underlying high-temperature superconductivity), it has been realized that the electron system in doped two-dimensional (2D) quantum Heisenberg antiferromagnets (AF) exhibits complicated ordering phenomena. On cooling from high temperatures, first a kind of phase separation is expected to occur, causing the formation of charged stripes separating mesoscopic AF domains [1–3]. In cuprates, in general, the stripes should exist only dynamically, with slowing down of their motions on cooling. At lower temperatures freezing of the spin degrees of freedom associated to the AF patches [4] causes the formation of a cluster spin-glass state [5–7]. Furthermore, there is evidence of unusual coupling of the lattice to charge and spin excitations [8]. For instance, ^{139}LaNMR line broadening, for $T \leq 40$ K, in $La_{2-x}Sr_xCuO_4$ (LSCO) for $x = 0.12$ (a signature of modulated magnetic order) is accompanied by softening of sound velocity [9]. Neutron diffraction, for $0 \leq x \leq 0.3$, indicates local tilts of octahedra, interpreted as evidence of charged stripes [10], the local tilt decreasing with increasing x.

[a] e-mail: campana@nmrvolta.unipv.it
andrea@nmrserver.unipv.it

In La_2CuO_4-based compounds, charge localization along stripes and spin freezing have been studied mostly by means of NMR-NQR and μSR spectroscopies [11,12]. In particular it has been argued [13] that, in the underdoped regime of LSCO, when diffraction experiments indicate complete ordering, the stripes are still fluctuating at low frequencies.

LSCO at Sr content around 0.02 is of particular interest, being at the boundary between the 3D-AF and the spin-glass phase [14]. Neutron scattering data [15] indicate that quasi-3D magnetic ordering occurs below about 40 K in the spin-glass state, with a spin structure related to the diagonal stripe structure.

Motivated by this scenario of interrelated lattice and spin fluctuation effects, we have carried out a comparative study of LSCO at $x = 0.02$ and $x = 0.03$ based on anelastic relaxation, ^{139}LaNQR spectra and relaxation.

Let us qualitatively recall how slowing down of spin fluctuations and ordering are expected to affect NQR and mechanical relaxation. Holes or charged stripes motions cause a time dependence in the hyperfine field $\mathbf{h}(t) = \sum_i \mathbf{A}_i \mathbf{S}_i(t)$ at the nucleus ($\mathbf{S}_i$ spin operator at the ith ion, $\mathbf{A}_i$ hyperfine coupling tensor). When a characteristic frequency ω_s becomes of the order of the NQR frequency $\omega_m = 2\omega_Q$ or $\omega_m = 3\omega_Q$ ($\omega_Q = 2\pi\, 6.2$ MHz), a maximum in the spin lattice relaxation rate W driven by the local time dependence of $\mathbf{h}(t)$ is expected. Below

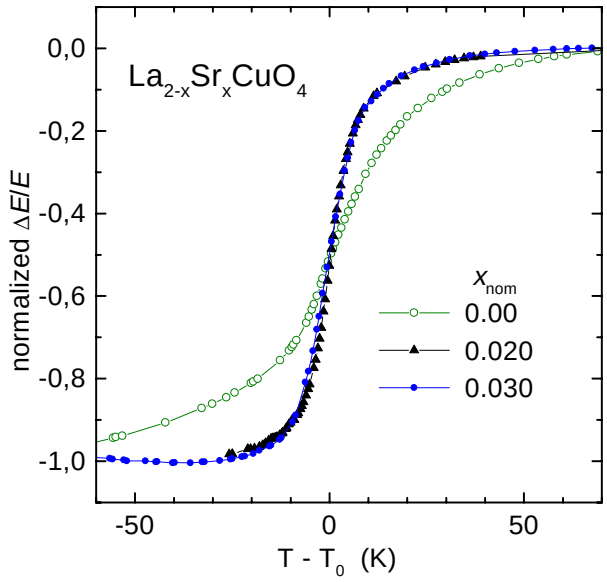

Fig. 1. Variation of the Young's modulus at the tetragonal orthorhombic transitions, normalized in amplitude and plotted as a function of $(T - T_0)$, with $T_0 = 535$ K for pure La_2CuO_4 and $T_0 = 495$ K and $T_0 = 468$ K for LSCO at $x = 0.02$ and $x = 0.03$ respectively, corresponding to the temperatures where half of the normalized variation of the Young modulus $\Delta E/E$ was observed.

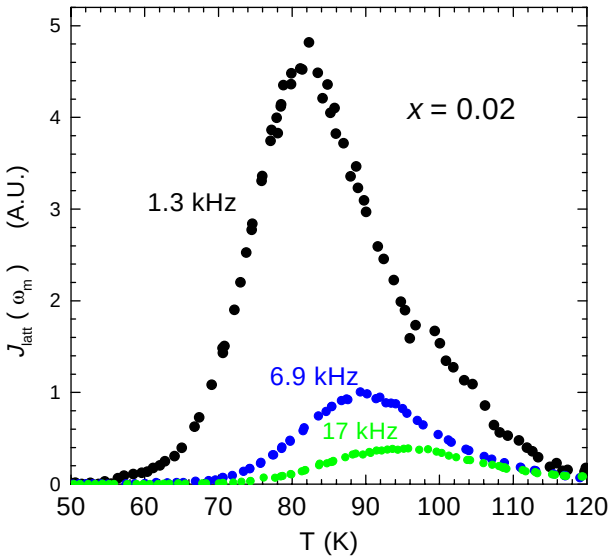

Fig. 2. Spectral density of the lattice motion responsible for the elastic energy loss coefficient in LSCO at Sr content $x = 0.02$ as a function of temperature, for three measuring frequencies.

this temperature the stripes move very slowly and local extra magnetic moments μ are induced, associated to the 2D patches of AF correlated regions [4]. On cooling, the cooperative slowing-down of these moments causes a second relaxation mechanism. As common for disordered systems, the correlation function for $\mu(t)$ can be written in the approximate form $\mu^2 \exp(-t/\tau_f(x,T))$, with an effective correlation time τ_f which increases on decreasing temperature. At the temperature $T_g(x)$ where τ_f becomes of the order of ω_m^{-1} another peak appears in W. In a long-range ordered AF matrix (in LSCO for $x \leq 0.02$) T_g should increase about linearly with x, due to the increased strength of the interaction among the μ_i's [6]. On the contrary, for an amount of doping x which destroys the long range AF order (cluster spin-glass phase) T_g decreases with increasing x [11,16,17]. Finally, μSR and ^{139}LaNQR measurements pointed out a magnetic transition to a spin-glass like phase well extending into the doping region yielding superconductivity in LSCO and YBCO [7,18].

As regards the effects expected in the anelastic relaxation, we recall the following. The elastic energy loss coefficient Q^{-1}, measured by exciting flexural vibrations, is given by $\frac{S''(\omega)}{S(\infty)}$, where $S(\omega)$ is the complex dynamics compliance with unrelaxed value $S(\infty)$. The contribution to the imaginary part of the mechanical susceptibility is thus given by $Q^{-1} \equiv [S''(\omega)/S(\infty)] \propto n[(\delta\lambda)^2/T]\omega J_{latt}(\omega)$ where n is the atomic fraction of relaxing units, each causing a change $\delta\lambda$ of the strain and $J_{latt}(\omega)$ is the spectral density of the motion causing dissipation [19].

Since the motions of the stripes involve sizeable lattice effects, when the characteristic frequency decreases down to the kHz range, a maximum in Q^{-1} is detected. Thus, from a combination of anelastic relaxation and of magnetic NQR relaxation, one can in principle probe the lattice and the spin fluctuations associated to the stripe motions. The investigation reported here was aimed at this purpose.

2 Experimentals results

Two LSCO ceramic samples grown by standard solid state reaction [20] have been investigated. According to X-ray diffraction the final amount of Sr were $x = 0.022$ and $x = 0.032$. A more precise estimate was obtained by detecting the orthorhombic-tetragonal transition in the Young modulus. The relationship of the transition temperature T_0 to the Sr amount was taken as $T_0(x) = 535[1 - (1/0.235)x]$ [14,21]. From the step in the Young modulus (Fig. 1) at the transition, one obtains $T_0 = 495$ K and $T_0 = 468$ K, corresponding to the Sr amounts $x = 0.019 \pm 0.0015$ and $x = 0.030 \pm 0.001$ (hereafter called samples 2 and 3 percent). The structural transition in LSCO appears even sharper than in pure La_2CuO_4 (where some broadening may be attributed to thermal de-oxygenation, which is less marked in Sr-doped compounds).

SQUID magnetization shows temperature behaviors typical of spin-glass systems. Small differences between the field cooled and zero-field cooled data below about 140 K have been attributed to magnetic impurities present in the powders used for the preparation. These impurities do not affect the ^{139}LaNQR and anelastic relaxation measurements.

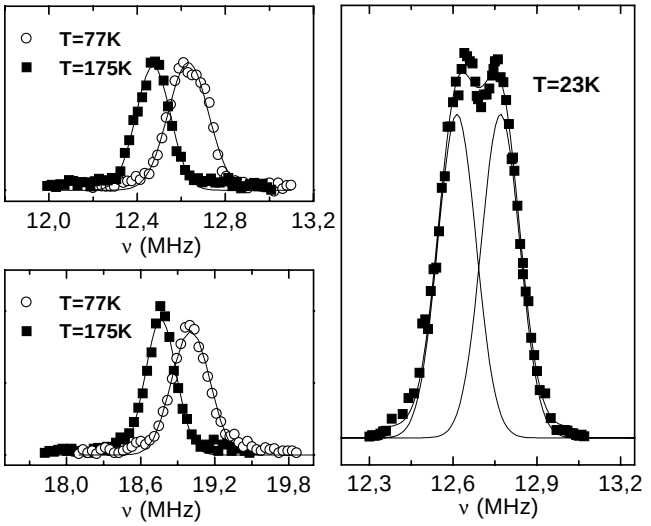

Fig. 3. ^{139}LaNQR spectra in LSCO at $x = 0.02$, at representative temperatures.

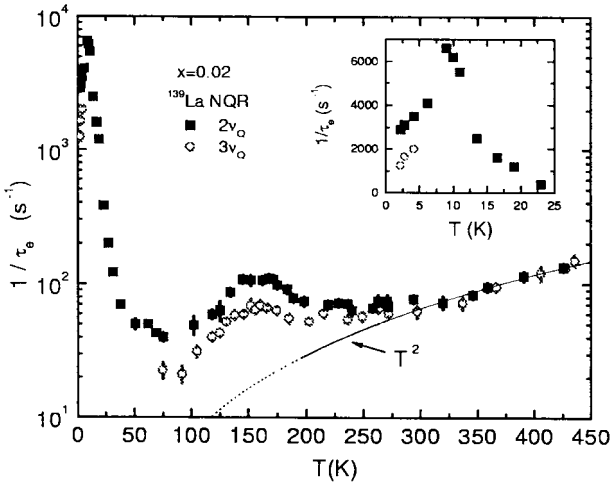

Fig. 4. Effective relaxation rates for ^{139}LaNQR relaxation in LSCO at $x = 0.02$, for the $3\nu_Q$ line and for the $2\nu_Q$ line. The inset is the blow up of the data for $T \leq 25$ K. The solid line is the sketch of the temperature dependence for relaxation driven by underdamped phonons.

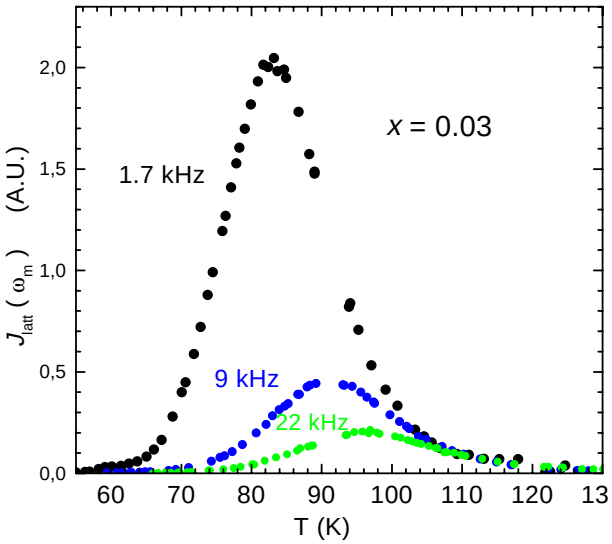

Fig. 5. Spectral densities of the motions responsible of the elastic energy loss in LSCO at $x = 0.03$, for three measuring frequencies.

In Figure 2 the spectral density of the motions causing dissipation, detected at the measuring frequencies $\omega/2\pi = 1.29$, 6.9 and 17.2 kHz, in LSCO at $x = 0.02$ are shown.

The ^{139}LaNQR spectra and relaxation rate have been measured by standard pulse techniques, irradiating the line at $2\nu_Q$ ($\pm 3/2 \leftrightarrow \pm 5/2$ transition) and the one at $3\nu_Q$ ($\pm 5/2 \leftrightarrow \pm 7/2$ transition). The NQR spectra have been obtained by sweeping the irradiation frequency ν_{RF}, Fourier transforming half of the echo signal and reporting the amplitude at $\nu = \nu_{RF}$. This procedure ensures the best resolution, avoiding any broadening related to the spectral width of the RF field.

^{139}LaNQR spectra for the $2\nu_Q$ and the $3\nu_Q$ lines at representative temperatures, at which we will refer in the discussion, are shown in Figure 3.

As regards ^{139}LaNQR relaxation measurements, it should be remarked that the recovery laws describing the return of the echo signal at the equilibrium after a fast RF sequence saturating the correspondent transition (without affecting the populations of the other NQR levels), are multiexponential. However in the first decade they differ only little from a single exponential. The correspondent effective decay rate τ_e^{-1} can easily be related to the magnetic relaxation rate W_M or to the quadrupolar relaxation rate W_Q due to the time dependence of the electric field gradients (EFG) at the La site [22]. In the case of relaxation driven by the electric quadrupole interaction one has

$$\begin{aligned} 3\nu_Q \text{ line} \quad & \tau_e^{-1} = (67/21) W_Q \\ 2\nu_Q \text{ line} \quad & \tau_e^{-1} = (64.5/21) W_Q \end{aligned} \qquad (1)$$

while in the case of relaxation driven by the time dependence of the magnetic hyperfine interaction one has

$$\begin{aligned} 3\nu_Q \text{ line} \quad & \tau_e^{-1} = 23\, W_M \\ 2\nu_Q \text{ line} \quad & \tau_e^{-1} = 41.3\, W_M. \end{aligned} \qquad (2)$$

The temperature dependence of the effective relaxation rates for LSCO 2 percent are reported in Figure 4.

In Figures 5 and 6 the temperature behaviours of $J_{latt}(\omega_m)$ and of the ^{139}LaNQR relaxation rates for the sample at Sr content $x = 0.03$ are reported.

3 Discussion and conclusions

Let us first analyse the experimental findings for anelastic relaxation (Fig. 2), in LSCO 2 percent. On physical ground one can expect that the motion responsible of the dissipation have cooperative character. For simplicity we neglect a possible frequency distribution and assign to the motion a single characteristic frequency ω_s. According to the data in Figure 2, the spectral density of these motions

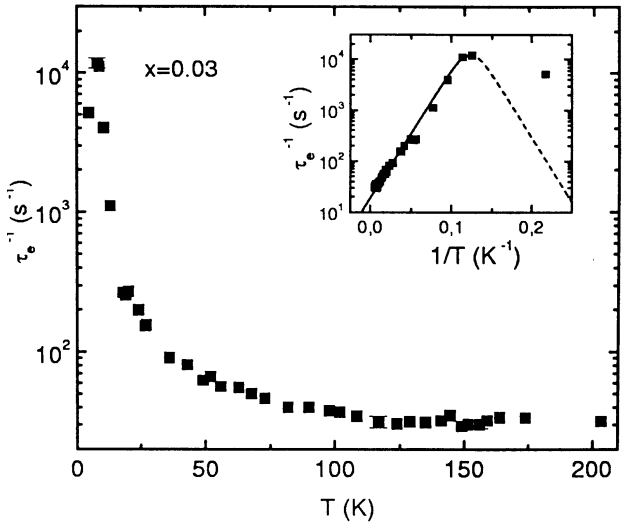

Fig. 6. ^{139}LaNQR relaxation rate for the $2\nu_Q$ line in LSCO at $x = 0.03$. In the inset the data for τ_e^{-1} are fitted according to the law $\tau_e^{-1} \propto \tau/(1+\omega_m^2\tau^2)$ with $\tau \propto \exp[E/T]$ with $E \simeq 58 \pm 2$ K.

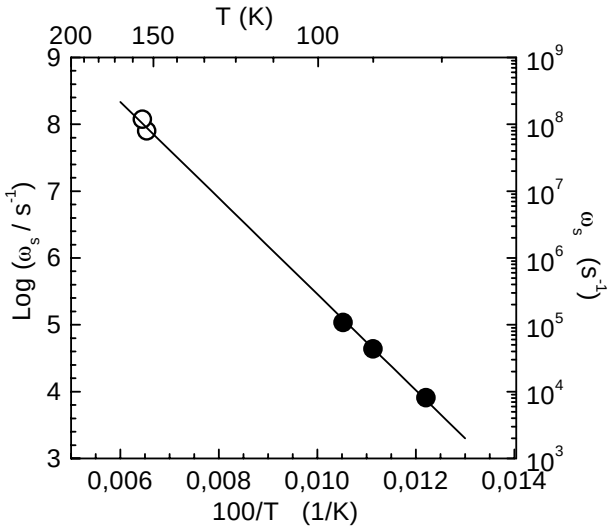

Fig. 7. Characteristic frequencies as estimated from the maxima in Figure 2 (solid circles). The line is the fitting behavior according to equation (4) in the text, with $\omega_0 = 4.5 \times 10^{12}$ s^{-1} and $E = 1650$ K. The empty circle are the frequencies deduced from the maxima in the ^{139}LaNQR relaxation rates, for $T \simeq 150$ K (Fig. 5).

has diffusive character:

$$J_{\rm latt}(\omega_m) = \frac{2\omega_s}{\omega_s^2 + \omega_m^2}. \qquad (3)$$

From the temperature where the maxima occur one can deduce the values of ω_s (solid circles in Fig. 7). A good fit of the data is obtained on the basis of a temperature behavior of ω_s of the form

$$\omega_s = \omega_0 \exp(-E/T) \qquad (4)$$

with $\omega_0 = 4.5\times10^{12}$ s^{-1} and $E = 1650$ K, indicating thermal activation of the motions.

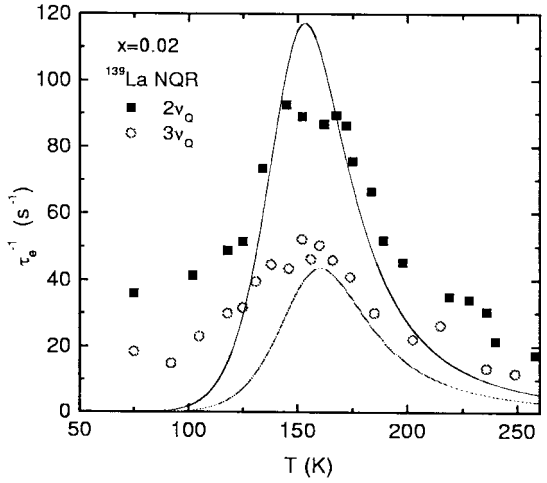

Fig. 8. NQR relaxation rates of magnetic origin obtained from the data in Figure 4 after the subtraction of the quadrupolar background contribution, in LSCO at $x = 0.02$, for the $3\nu_Q$ and the $2\nu_Q$ line. The solid lines are the theoretical behaviors according to equation (6) in the text ($|h|^2$ as adjustable parameter) by using for ω_s the form deduced from anelastic relaxation (Eq. (4) in the text).

The motions involving lattice dissipation are expected to cause also time dependence in the hyperfine field $\mathbf{h}(t) = \sum_i \mathbf{A}_i\mathbf{S}_i(t)$ at the nucleus and/or in the EFG component driving the ^{139}LaNQR relaxation process. This correspondence between mechanical and NQR relaxation has been recently demonstrated [19] in pure La_2CuO_4, in terms of the overdamped phonon modes describing the tilting of the oxygen octahedra in a double well potential.

For $T \geq 250$ K the ^{139}LaNQR relaxation rates reported in Figure 4 are frequency independent and follow the law $\tau_e^{-1} \propto T^2$ (solid line in Fig. 4). These features are characteristic of relaxation process driven by underdamped phonon [23]. An order of magnitude estimate corroborates this conclusion, since for this process one expected $\tau_e^{-1} \simeq 5 \times 10^{-4} T^2$ s^{-1} [24]. The contribution from overdamped tilting modes is strongly attenuated in Sr-doped La_2CuO_4, as indicated by anelastic relaxation measurement [25]. Some evidence of such a contribution can be noted around $T \simeq 280$ K in Figure 4. Below 250 K τ_e^{-1} depart from the behavior for relaxation driven by EFG fluctuations. For temperatures lower than about 180 K infact the comparison of the data for the $3\nu_Q$ and $2\nu_Q$ lines indicates the insurgence of a *magnetic* relaxation mechanism. The behavior of τ_e^{-1} for $T \leq 230$ K is analyzed in detail in Figure 8, after subtraction of the background of quadrupole character. Assuming that the modulation of the hyperfine field $\mathbf{h}(t)$ is due to the same motion causing the mechanical relaxation, then for

$$2W_M = \frac{1}{2}\gamma^2 \int \langle h_+(0)h_-(t)\rangle e^{-i\omega t} dt, \qquad (5)$$

from equations (2) and (3) one can write

$$(\tau_e^{-1})_{3\nu_Q} = \frac{23}{2}\gamma^2|h|^2[2\omega_s/(\omega_s^2 + (3\omega_Q)^2)]$$

$$(\tau_e^{-1})_{2\nu_Q} = \frac{41.3}{2}\gamma^2|h|^2[2\omega_s/(\omega_s^2 + (2\omega_Q)^2)] \qquad (6)$$

where $|h|^2$ is an effective mean square value of the field coupling the Cu^{2+} ions to the La nucleus [12]. In Figure 8 the experimental data for τ_e^{-1}'s are compared with the theoretical behaviors for the relaxation rates according to equations (6), having used for ω_s the expression derived from the anelastic relaxation (Eq. (4)). The maxima are well reproduced. The departures of the experimental data from the theoretical expressions in the temperature range corresponding to slow motions, *i.e.* $\omega_s \leq \omega_m$, are likely to be due to the simplifying assumption of a monodispersive process. Infact, a distribution in ω_s implies a flattening in the relaxation rate around the maximum and a departure from the behavior for monodispersive process more marked in the low temperature range, as it appears in the figure. The relevant fact is that the temperature dependence of ω_s deduced from anelastic relaxation in the kHz range supports quantitatively the magnetic NQR relaxation rate in the MHz range.

In view of the uncertainty in the phase diagram for Sr-doped La_2CuO_4 around the "critical" value $x = 0.02$, one should take into account the possibility that the maxima in $\tau_e^{-1} \propto W_M$ around 150 K reflect the slowing down of spin dynamics on approaching the transition to an ordered state. Information in this regard can be obtained from the NQR spectra, since the insurgence of a static field $\langle h \rangle$ at the La site is signaled by a splitting Δ of the resonance line, proportional to the sublattice magnetization $\langle S \rangle$. A clear splitting of the line is noticeable only below about 50 K, close to the transition temperature indicated by neutron scattering [15]. If the width δ of a single component is kept temperature independent the fitting of the spectra with two Gaussian lines yields an ordering temperature T_N, where Δ goes to zero, of about 140 K. The temperature dependence of the order parameter $\langle S \rangle \propto \langle h \rangle$ would turn out quite different from the one of a canonical phase transition to the AF phase, experimentally observed [26] in pure La_2CuO_4.

On the other hand, if the maxima in W_M at 150 K are taken as an indication of stripe motion at frequency around ω_Q, then NQR line broadening must be expected below the temperature at which the frequency becomes of the order of the line width itself, about 200 kHz, namely around 110 K according to Figure 7. An experimental support to the hypothesis that the intrinsic linewidth δ is temperature dependent comes from the comparison of the spectra at $2\nu_Q$ and at $3\nu_Q$ (Fig. 3). The ratio $\delta_{2\nu_Q}(T = 77\ \text{K}) / \delta_{2\nu_Q}(T = 177\ \text{K}) = (210\ \text{kHz}) / (183\ \text{kHz}) = 1.15$ is the same as the one for the $3\nu_Q$ line: $\delta_{3\nu_Q}(T = 77\ \text{K}) / \delta_{3\nu_Q}(T = 177\ \text{K}) = (320\ \text{kHz}) / (280\ \text{kHz}) = 1.15$. One also has $\delta_{3\nu_Q} = (3/2)\,\delta_{2\nu_Q}$. These data are not compatible with an effect due to a magnetic field $\langle h \rangle$, that would cause an extra broadening of the same amount for both the $2\nu_Q$ and the $3\nu_Q$ lines. Thus, if a moderate (of the order of 15–20%) temperature dependence for the single component linewidth δ is allowed, then the NQR spectra indicate $T_N \simeq 50$ K. This value is in substantial agreement with the phase diagram commonly accepted in literature [14]. One could speculate that at this temperature a small bump, consistent with slowing-down of spin dynamics, is observed in the relaxation rates (Fig. 4). On cooling, the relaxation rate exhibits a maximum at a temperature around $T = 9$ K, due to the spin freezing. Also the recovery plots, showing evidence of departure from an exponential recovery towards the $t^{1/2}$ law, support the conclusion that the spin-glass quasi-freezing temperature has been reached.

We compare now the experimental findings in the sample at the boundary between the AF and the spin-glass phase with the one at $x = 3$ percent, well within the latter phase. The anelastic relaxation shows a temperature behavior similar to the one for $x = 2$ percent (Fig. 5). The peaks attributed to the stripes motion are attenuated by a factor of about two. The ^{139}LaNQR relaxation rates (Fig. 6) indicate the typical freezing of the spin fluctuations in a spin-glass state. The maximum in W_M occurs at $T = 8$ K, in agreement with the phase diagram by Cho *et al.* [16,21].

The relaxation rate measured at $2\nu_Q$ reaches a value about twice the one reported in previous measurements [16,27,28] at $3\nu_Q$, consistent with a magnetic relaxation mechanism. The temperature behavior of τ_e^{-1} is rather well fitted by a correlation time of the form $\tau \propto \exp[E/T]$, the departure of the data for $T < T_g$ (slow motion regime) resulting from the distribution of τ's, typical of the spin-glass state. One should remark that for $x = 0.03$ also magnetic measurements [29] yield evidence of the occurrence of a canonical spin-glass state. One the contrary, the relaxation data in the sample $x = 0.02$ (see inset in Fig. 4) can hardly be described by a temperature behavior of τ of the form $\tau \propto \exp[E/T]$, again pointing out the particular character of this "critical" concentration.

In summary, in this paper, anelastic and NQR relaxation and NQR spectra have been combined in the attempt to derive insights on spin and lattice excitations driving the ordering processes in LSCO. The experimental findings have been discussed within two interpretative frameworks. On one side it could be possible that the phase diagram around the Sr content $x = 0.02$ separating the AF and the spin-glass phases is more complex that previously assumed, with a quasi-long range ordering temperature as high as 150 K, corroborating recent neutron scattering measurements [15] and qualitatively agreeing with the extrapolation at $x = 0.02$ of a magnetization study [29] carried out in samples at $x = 0.03$, 0.04 and 0.05. The order parameter of such a transition, derived from the splitting of the ^{139}LaNQR line, would be characterized by an unconventional temperature dependence.

On the other hand, the NQR spectra can be interpreted as indicating a transition to the AF phase around $T = 50$ K, in agreement with the phase diagram commonly accepted. In this case the anelastic and La NQR relaxation rates around $T = 80$ K and $T = 150$ K respectively, are the first direct experimental evidence of low frequency motions of charged stripes simultaneously involving spin and lattice excitations. The thermal depinning barriers and the characteristic "diffusive" frequencies are then derived,

and they do not differ much for Sr content 0.03. In the low temperature range a spin freezing process is detected, with a dramatic increase of the ^{139}LaNQR relaxation rate on cooling, a stretched exponential recovery and a low temperature behavior of the relaxation rate typical of a cluster spin glass phase for $x = 0.02$ and of a canonical spin glass for $x = 0.03$.

Alessandro Lascialfari is gratefully thanked for the SQUID measurements and for helpful discussions. Stimulating discussions with F. Borsa, P. Carretta, R. Gooding and M.H. Julien are acknowledged. The research has been carried out in the framework of the PRA project SPIS (1998-2000), financed by INFM (Italy).

References

1. See several papers in the Proceedings of the 1996 and 1998 Rome Conferences on "Stripes and High-T_c Superconductivity", J. Superconductivity **10** (4) (1997, 1999).
2. J. Zaanen, O. Gunnarson, Phys. Rev. B **40**, 7391 (1989).
3. V.J. Emery, S. Kivelson, Physica C **209**, 597 (1993); J. Phys. Chem. Solids **59**, 1705 (1998).
4. R.J. Gooding *et al.*, Phys. Rev. B **55**, 6360 (1997).
5. A. Weidinger *et al.*, Phys. Rev. Lett. **62**, 102 (1989).
6. F.C. Chou *et al.*, Phys. Rev. Lett. **71**, 2323 (1993).
7. Ch. Niedermayer *et al.*, Phys. Rev. Lett. **80**, 3843 (1998).
8. For a review, see T. Egami, S.J.L. Billinge, *Lattice Effects in High-Temperature Superconductors*, in *Physical Properties of High-Temperature Superconductors V*, edited by D.M. Ginsberg (World Scientific, 1998). A phase diagram for the stripes dynamics in terms of lattice potential has been recently discussed by C. Morais Smith *et al.*, `cond-mat/9912074` (1999).
9. T. Suzuki *et al.*, Phys. Rev. B **57**, 3229 (1998).
10. E.S. Bozin *et al.*, Phys. Rev. B **59**, 4445 (1999).
11. F. Borsa *et al.*, Phys. Rev. B **52**, 7334 (1995).
12. For a review, see A. Rigamonti, F. Borsa, P. Carretta, Rep. Progress Phys. **61**, 1367 (1998).
13. A.W. Hunt, P.M. Singer, K.R. Thurber, T. Imai, Phys. Rev. Lett. **82**, 4300 (1999).
14. D.C. Johnston, in *Handbook of Magnetic Materials*, Vol. 10, edited by K.H.J. Buschow (Elsevier Science, North Holland, 1997), p. 1.
15. M. Matsuda *et al.*, Phys. Rev. B **61**, 4326 (2000).
16. J.H. Cho *et al.*, Phys. Rev. B **46**, 3179 (1992).
17. P. Carretta, F. Cintolesi, A. Rigamonti, Phys. Rev. B **48**, 7044 (1994).
18. M.-H. Julien *et al.*, Phys. Rev. Lett. **83**, 604 (1999).
19. F. Cordero, R. Cantelli, M. Corti, A. Campana, A. Rigamonti, Phys. Rev. B **59**, 12078 (1999).
20. The samples have been prepared and characterized by X-ray diffraction by M. Ferretti and coworkers (Dep. of Chemistry, University of Genova).
21. J.H. Cho, F.C Chou, D.C. Johnston, Phys. Rev. Lett. **70**, 222 (1993).
22. T. Rega, J. Phys. C **3**, 1871 (1991).
23. A. Rigamonti, Adv. Phys. **33**, 115 (1984).
24. In this estimate the phonon frequency of 3 meV and a width of the optical branch of 8 meV derived from neutron scattering (R.J. Birgeneau *et al.*, Phys. Rev. Lett. **59**, 1329 (1987)) have been used (see Borsa *et al.*, Nuovo Cimento D **11**, 1785 (1989)).
25. F. Cordero *et al.*, Phys. Rev. B **61**, 9775 (2000).
26. D.E. MacLaughlin *et al.*, Phys. Rev. Lett. **72**, 760 (1994).
27. F. Borsa, M. Corti, T. Rega, A. Rigamonti, Nuovo Cimento D **11**, 1785 (1989).
28. A. Rigamonti *et al.*, in *Early and recent aspects of superconductivity*, edited by J.G. Bednorz, K.A. Muller (Springer, 1991) p. 441.
29. S. Wakimoto *et al.*, `cond-mat 9910400` (1999).